An IoT Distributive SM Controller for Mitigation of Circulating Currents Among Sources in a Standalone DC Microgrid

Muhammad Sharjeel Sarwar[1], Muhammad Rashad[1], Tayybah Kiren[2], Nazam Siddique[3], Bilal Ishfaq Ahmed[4], Adeel Ahmed[1], Muhammad Wasif[3], Muhammad Jehanzeb Irshad[3]
[1]Department of Electrical Engineering (The University of Lahore (UOL), Lahore, Pakistan).
[2]Department of Computer Science (University of Engineering and Technology (UET), Lahore, Pakistan).
[3]Department of Electrical Engineering (University of Gujrat (UOG), Gujrat, Pakistan).
[4]Department of Informatics and Systems (University of Management and Technology (UMT), Lahore, Pakistan).
***Correspondence:** muhammad.rashad@ee.uol.edu.pk

Citation | Sarwar. M. S, Rashad. M, Kiren. T, Siddique. N, Ahmed. B. I, Ahmed. A, Wasif. M, Irshad. M. J, "An IoT Distributive SM Controller for Mitigation of Circulating Currents Among Sources in a Standalone DC Microgrid", IJIST, Special Issue. pp 274- 287, March 2025.
Received Feb 27, 2025 **Revised|** March 11, 2025 **Accepted|** March 17, 2025 **Published|** March 20, 2025.

Sources of similar or different power ratings are connected in parallel within the DC microgrid. During operation, these sources generate circulating currents along with their normal currents, which disrupt proper current sharing among power electronic converters based on their capacity. Consequently, voltage regulation across the system weakens. Additionally, the resistance of the connecting lines contributes to this imbalance in current distribution. To address circulating currents, droop controllers are commonly used. This method allows converters to share power according to their capacity without requiring internal communication. However, a major drawback of conventional droop control is that as output voltage decreases, the converter's output current increases linearly, leading to significant voltage fluctuations. As a result, droop control inherently involves a trade-off between voltage regulation and current sharing, making it impossible to optimize both simultaneously. To overcome this issue, this paper proposes a sliding mode (SM) controller implemented through an IoT-based distributed architecture. A system model is developed to evaluate its performance, and conditions for stability and existence are analyzed. MATLAB simulations provide detailed experimental results, demonstrating the effectiveness of the proposed technique.

Keywords: Droop Control; Circulating Currents; Voltage Regulation; Sliding Mode Controller; Existence Condition; Stability Condition.

Introduction:

In the modern era, microgrids are self-sufficient, small-scale power systems that can generate and consume electricity independently. They can also exchange power with other microgrids and the utility grid based on demand. From a design perspective, microgrids are classified as AC, DC, or Hybrid. In terms of control architecture, they can be categorized as decentralized, centralized, or distributed [1][2][3][4].

The development of microgrids, particularly in distributed generation, creates new opportunities for utilizing renewable energy sources (RESs). This advancement can play a crucial role in electrifying underdeveloped regions, helping them bridge the gap with developed and emerging nations. A reliable communication system is essential for microgrids, ensuring complete and bidirectional connectivity between resources while maintaining interoperability. Additionally, a new generation of peer-to-peer communication schemes is expected to enhance the efficiency and functionality of modern microgrids [5][6][7].

Microgrids are classified as AC or DC based on their operational format. AC microgrids integrate various energy sources and loads using an AC bus system. In these systems, DC-AC and AC-DC conversions are necessary to support DC loads. Similarly, DC microgrids operate comparably to AC microgrids, with the key difference being the use of a DC bus for interconnection [8].

DC microgrids are becoming increasingly popular due to their high efficiency, reliability, and ease of integrating renewable energy sources compared to AC microgrids. Additionally, DC systems eliminate issues such as skin effect, reactive power, frequency regulation, and synchronization, making them a highly dependable and promising solution for future energy needs [9]. Table 1 provides a brief comparison between AC and DC microgrids.

Table 1 Comparison of AC and DC microgrids

Factors	AC	DC
Converter requirement [6], [8], [10]	More Converters	Fewer Converters
Power Requirement [7][8]	Complex Power	Only Active Power
Power Factor Issues [7][8]	Yes	No
Stability [8], [11][10]	Low	High
Microgrid Controls [11][10]	Complex	Simple
Protection [7][8]	Low Cost	High Cost
Reactive Power Compensation [7]	Required	Not Required
Frequency Synchronization [8], [11][10]	Required	Not required

Precise current sharing and voltage regulation are essential in DC microgrids, especially when sources are connected in parallel. The current-sharing issue arises due to circulating currents, which result from differences in output voltage and cable resistance. These circulating currents must be minimized or eliminated to ensure proper current distribution. A well-designed control strategy should maintain system stability while achieving the desired performance.

Control schemes for DC microgrids fall into three categories: decentralized, centralized, and distributed. Some power flow control methodologies, based on hierarchical layers for control parameter flow and decision-making, are discussed in [11], while hierarchical control methods are explored in detail in [10]. Power electronic converters are key components in every DC microgrid, and their challenges are highlighted in [12].

A parallel DC-DC converter arrangement offers several advantages over a single high-capacity centralized converter. These benefits include increased reliability, improved efficiency, enhanced thermal management, lower maintenance, and reduced stress on individual converters, as the total load current is distributed among them [13]. However, despite these advantages, proper control strategies are necessary to regulate load voltage and

ensure precise load sharing among converters [14]. Uneven current distribution can cause overheating, potentially leading to system failure. Research shows that the main challenge in parallel-connected DC-DC converters is ensuring both voltage regulation and accurate current sharing. While centralized controllers can achieve these objectives, they require high-bandwidth communication, making them vulnerable to single-point failures. To overcome these limitations, a decentralized control architecture for DC microgrids is presented in [15]. Although it simplifies system design, it lacks information on parallel sources, preventing simultaneous load sharing and voltage regulation. Thus, decentralized control is not ideal for DC microgrid applications.

Current-sharing control methods are mainly categorized into droop control and active-sharing techniques. In islanded DC microgrids, droop control is the most commonly used method for stabilizing bus voltage when parallel converters operate without communication [16]. Droop techniques involve adding virtual resistance to the output voltage of all converters. As a result, each converter's output voltage decreases, increasing the load current. While simple and decentralized, droop control often leads to poor voltage regulation. Reducing droop gain improves voltage regulation but compromises accurate load sharing. Increasing droop gain beyond cable resistance can enhance current sharing, but this results in significant voltage deviations from no-load to full-load conditions.

In contrast, active current-sharing methods typically use a dual-loop control structure with an outer voltage control loop and an inner current control loop. These loops are decoupled based on frequency considerations [17]. However, variations in bandwidth and frequency separation can affect transient performance and overall system stability. A master-slave current-sharing control strategy for parallel power electronic converters is discussed in [18], where the master converter retains its characteristics while slave converters function as current-controlled current sources.

A cooperative distributed control strategy for voltage regulation and current sharing in parallel DC converters is presented in [19]. This method does not require knowledge of the number of converters. Another distributed control approach, which ensures average voltage regulation and current sharing through resistive-inductive electrical lines, is detailed in [20]. Distributed control allows simultaneous load sharing and voltage regulation, but conventional PI-based control techniques pose challenges. Classical controllers struggle with parameter tuning, adapting to load variations, and achieving stability under all conditions, making them less suitable for DC microgrid applications.

The rest of this paper is structured as follows: Section 2 formulates the equations for circulating currents and control architectures using voltage-only and cascaded voltage-current loops. Section 3 introduces the proposed SM controller and IoT-based distributed architecture, along with stability and existence conditions. Section 4 presents the results and discussion, while Section 5 concludes the paper.

Research Objectives:

The primary objective of this research is to minimize circulating currents among parallel-connected sources in a DC microgrid. The second objective is to achieve simultaneous load sharing and precise voltage regulation.

Novelty Statement:

Existing control techniques fail to achieve both load sharing and voltage regulation simultaneously. To overcome this challenge, this paper proposes an IoT-based distributed architecture using a robust SM controller. In the SM controller, voltage and current loops are processed simultaneously. To evaluate its performance, a system model is developed, and the existence and stability conditions of the SM controller are analyzed. MATLAB simulation results are presented to demonstrate the effectiveness of the proposed technique.

Material and Methods:

System Modelling:

The basic structure of the DC microgrid is shown in Fig. 1. All RESs are either direct DC sources or DC-compatible. The main utility grid and wind turbines generate AC power, which is connected to the DC bus through an AC-DC converter [21]. A single arrow indicates unidirectional power flow for loads, PV arrays, and fuel cells, while battery energy storage systems (BESS) and the conventional utility grid exhibit bidirectional power flow, meaning they can both supply and consume power.

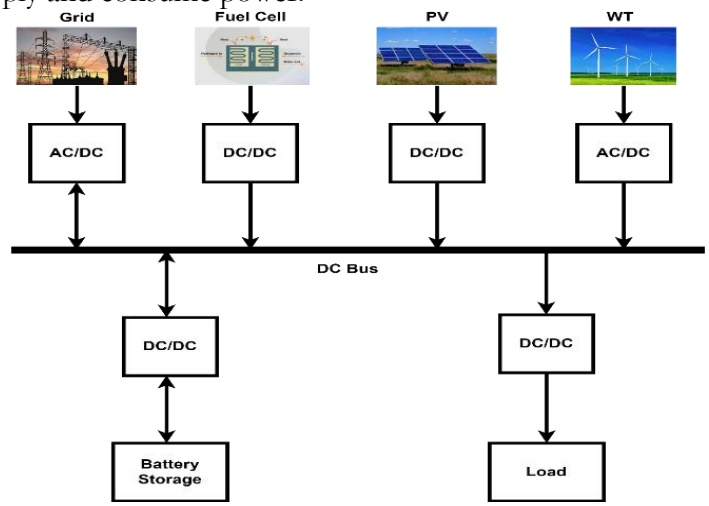

Figure 1 Typical arrangement of a DC microgrid.

A DC microgrid with two parallel sources connected to a load through a DC bus is shown in Fig. 2. Here, R_1 and R_2 represent the cable resistances, while i_{dc1} and i_{dc2} are the currents shared by the two sources, which have terminal voltages v_{dc1} and v_{dc2}, respectively.

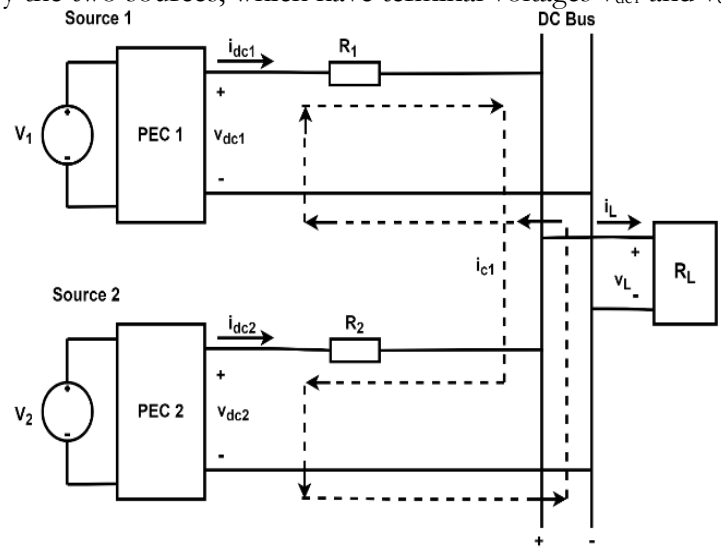

Figure 2 Two sources connected in a parallel configuration.

Formulation of Circulating Current Equations:

A steady-state equivalent network of the DC microgrid from Fig. 2 is illustrated in Fig. 3. Here, v_{dc1} and v_{dc2} represent the terminal voltages of sources 1 and 2, while the interconnecting cables are modeled by resistances R_1 and R_2, respectively. Applying Kirchhoff's Voltage Law (KVL) to loop 1, as shown in Fig. 3, the equations for v_{dc1} and v_{dc2} can be expressed as follows in (1) and (2):

$$v_{dc1} = i_{dc1}R_1 + i_L R_{Load} \quad (1)$$

$$v_{dc2} = i_{dc2}R_2 + i_L R_{Load} \quad (2)$$

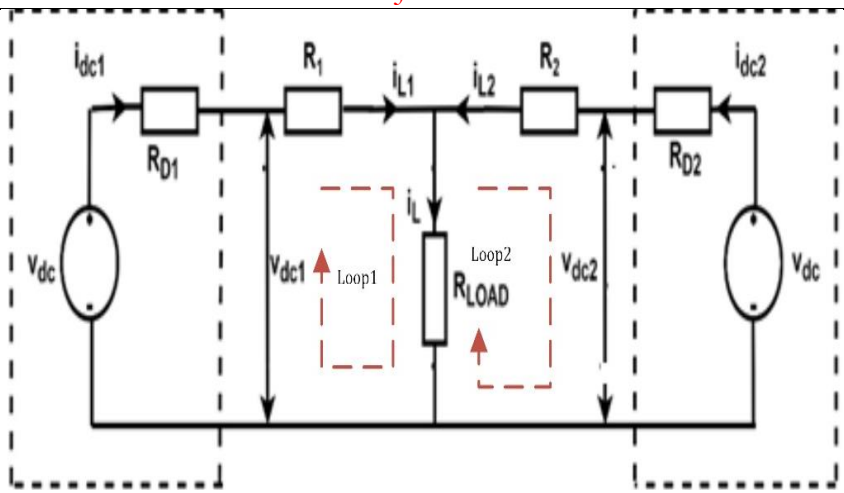

Figure 3 Steady-state equivalent circuit of two parallel connected sources.

Here, i_{dc1} and i_{dc2} are the currents supplied by sources 1 and 2, respectively, while i_t represents the load current. These currents are mathematically related as:

$$i_L = i_{L1} + i_{L2} \quad (3)$$

$$i_{dc1} = i_{L1} + i_{c1} \quad (4)$$

$$i_{dc2} = i_{L2} + i_{c2} \quad (5)$$

Here, i_{c1} and i_{c2} are the circulating currents of sources 1 and 2, respectively. These currents have the same magnitude but flow in opposite directions [22]. To determine i_{dc1} and i_{dc2}, equations (3), (4), and (5) are substituted into (1) and (2). After simplification, i_{dc1} and i_{dc2} can be expressed in the form of equations (6) and (7).

$$i_{dc1} = \alpha_1 v_{dc1} - \beta v_{dc2} \quad (6)$$

$$i_{dc2} = \alpha_2 v_{dc2} - \beta v_{dc1} \quad (7)$$

Were,

$$\alpha_1 = \frac{R_2 + R_{LOAD}}{R_1R_2 + R_2R_{LOAD} + R_1R_{LOAD}} \quad (8)$$

$$\alpha_2 = \frac{R_1 + R_{LOAD}}{R_1R_2 + R_2R_{LOAD} + R_1R_{LOAD}} \quad (9)$$

$$\beta = \frac{R_{LOAD}}{R_1R_2 + R_2R_{LOAD} + R_1R_{LOAD}} \quad (10)$$

The product R_1R_2 in equations (8), (9), and (10) can be neglected, as its value is very small compared to the load resistance R_{LOAD}. Similarly, to determine i_{c1} and i_{c2}, equations (6) and (7) are substituted into equations (4) and (5). After simplification, i_{c1} and i_{c2} can be expressed in the form of equation (11).

$$i_{c1} = -i_{c2} = \frac{v_{dc1} - v_{dc2}}{R_1 + R_2} = \frac{i_{dc1}R_1 - i_{dc2}R_2}{R_1 + R_2} \quad \text{if } (R_1 \neq R_2)$$

$$= \frac{i_{dc1} - i_{dc2}}{2} \quad \text{if } (R_1 = R_2) \quad (11)$$

Substituting equation (11) into equations (4) and (5) gives equations (12) and (13).

$$i_{dc1} = \frac{R_2 v_{dc2}}{R_1R_{LOAD} + R_2R_{LOAD}} + \frac{v_{dc1} - v_{dc2}}{R_1 + R_2} \quad (12)$$

$$i_{dc2} = \frac{R_1 v_{dc1}}{R_1R_{LOAD} + R_2R_{LOAD}} - \frac{v_{dc2} - v_{dc1}}{R_1 + R_2} \quad (13)$$

In equations (12) and (13), the first part is the load current, and the second part is the

circulating current. Similarly, the analysis of the circulating current for any number of parallel-connected sources can be extended.

In equations (12) and (13), the first term represents the load current, while the second term corresponds to the circulating current. Similarly, this circulating current analysis can be extended to any number of parallel-connected sources.

Control Methods of DC Microgrid:

Several control methods in the literature use PI controllers to mitigate circulating currents and regulate voltage in DC microgrids. A simple voltage control loop for a source-j is shown in Fig. 4. Here, the output voltage V_{oj} is compared with the reference voltage V_j^{ref}, and the error is processed by a PI controller to generate a Pulse Width Modulation (PWM) signal for regulating the Power Electronic (PE) converter. However, this method is only suitable for voltage regulation and does not minimize circulating currents.

A cascaded voltage and current loop method using a PI controller is shown in Fig. 5. In this approach, the voltage error regulates the output voltage, while the current error controls the current shared by the sources. However, since these control techniques are linear, they cannot ensure stability in all operating conditions, making it difficult to minimize circulating currents effectively.

To overcome this limitation, the next section introduces a nonlinear SM control technique to minimize circulating currents among sources.

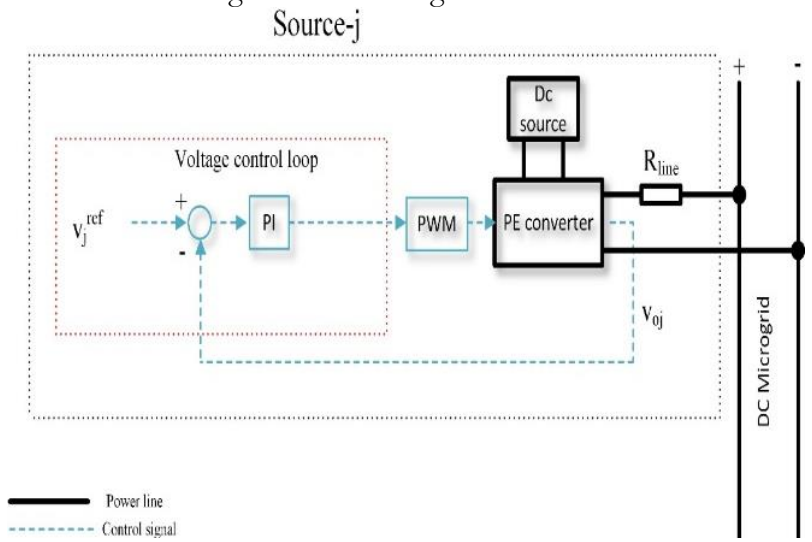

Figure 4 PI control of DC microgrid via voltage loop.

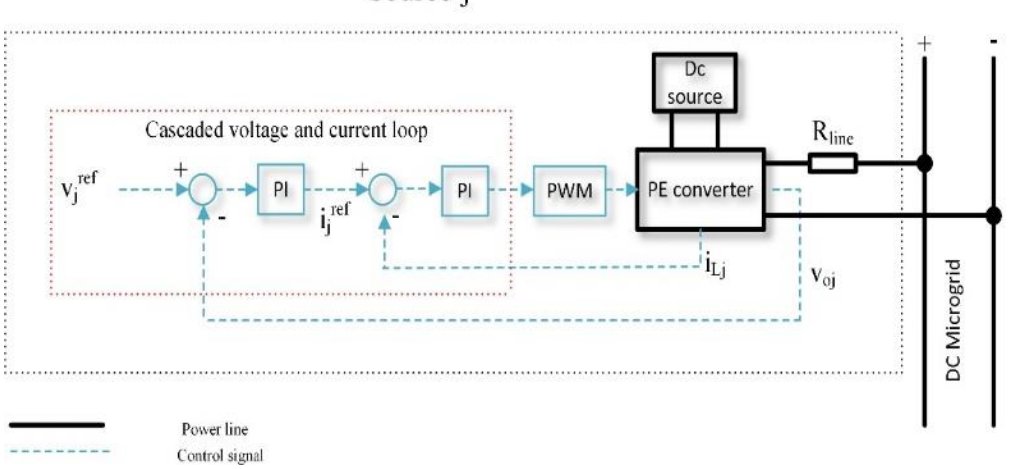

Figure 5 PI control of DC microgrid via cascaded voltage and current loop.

Proposed Sliding Mode Control:

The Sliding Mode (SM) controller is a nonlinear control method designed specifically for variable-structure systems, ensuring robustness and stability under all operating conditions. Fig. 6 illustrates the block diagram of a DC microgrid controlled using the SM controller.

In SM operation, both voltage and current loops function in parallel, enabling a fast dynamic response. The switched differential equations of the Power Electronic (PE) buck converter, which describe the system's state dynamics, are presented in equations (14) and (15). These equations form the basis for designing the SM controller.

$$\frac{dv_o}{dt} = \frac{i_L - i_{Line}}{C} \quad (14)$$

$$\frac{di_L}{dt} = \frac{uv_i - v_o}{L} \quad (15)$$

Here, i_L and i_{Line} Represent the inductor current and the connecting line current, respectively. Similarly, v_i and v_o Denote the input and output voltages. The capacitance and inductance are represented by C and L, respectively.

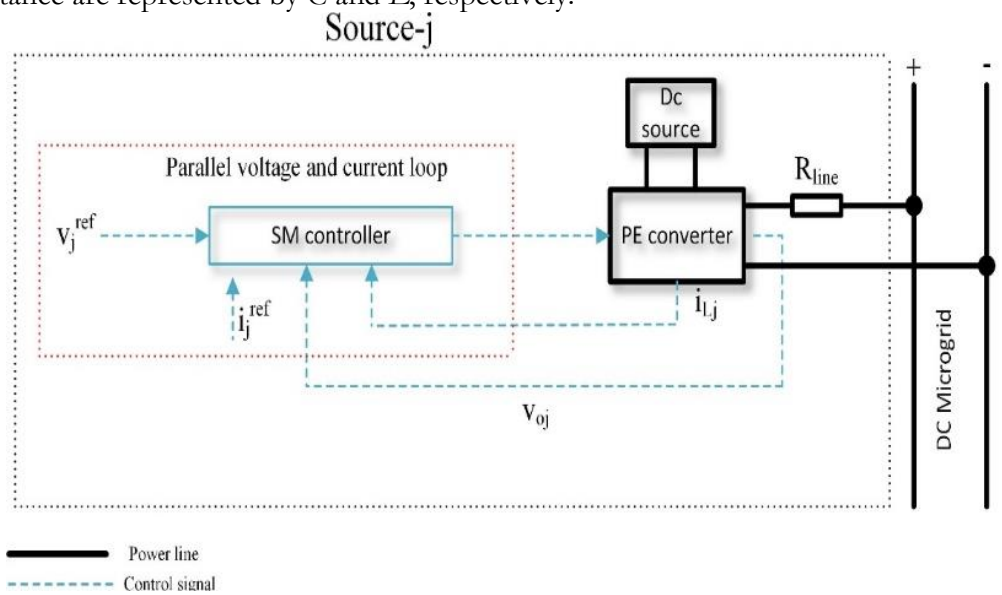

Figure 6 SM controller for parallel-connected DC microgrid.

SM Controller Design:

The sliding manifold in this paper is designed using the DC voltage error and converter current error. The SM controller identifies circulating currents by analyzing these errors. The proposed sliding surface is mathematically expressed in equation (16), where:

- $e_v = v_{ref} - v_o$ Represents the DC voltage error.
- $e_i = i_{ref} - i_L$ Represents the converter's current error.
- α and β are the sliding surface constraints.

$$\varphi = \alpha e_v + \beta e_i \quad (16)$$

The differentiation of the sliding function provides insight into the system's dynamic behavior and control response. It is mathematically represented in equation (17), showing how the sliding function evolves.

$$\frac{d\varphi}{dt} = -\alpha \frac{dv_o}{dt} - \beta \frac{di_L}{dt} \quad (17)$$

By substituting the derivatives of the output voltage and load current from equations (14) and (15) into equation (17), we obtain equation (18), which expresses the dynamics of the sliding function in terms of system parameters.

$$\frac{d\varphi}{dt} = \frac{-\alpha(i_L - i_{Line})}{C} - \frac{\beta(uv_i - v_o)}{L} \quad (18)$$

The equation (18) is used to define the transversality condition, which ensures that the sliding mode controller effectively influences the system's dynamics. This condition is mathematically expressed as:

$$\frac{d\varphi}{du} \neq 0 \quad (19)$$

This guarantees that the system does not remain in a singularity where control actions become ineffective.

The reachability condition ensures that the system states always move toward and remain on the sliding surface. Mathematically expressed as:

$$\varphi \frac{d\varphi}{dt} < 0$$

This ensures that any deviation from the sliding surface is corrected, forcing the system toward the desired operating point and maintaining stability.

Transversality Condition:

The transversality condition ensures that the control input appears explicitly in the sliding surface derivative, allowing the controller to influence system dynamics. Mathematically, this condition can be expressed as:

$$\frac{d\varphi}{dt} = f(x) + g(x)u$$

Where:

- *f(x)* represents the system dynamics without control input.
- *g(x)u* represents the influence of the control input u.

This guarantees that the controller can effectively drive the system states to the sliding surface and maintain stability. Substituting the value of $\frac{d\varphi}{dt}$ From equation (18) into equation (19) results in the equation (18).

$$\frac{d\frac{d\varphi}{dt}}{du} = \frac{-\beta}{L} v_i \quad (20)$$

The result in equation (20) confirms that the control input explicitly appears in the system dynamics, ensuring that the modeled system is controllable.

Reachability Condition:

The reachability conditions ensure that the system trajectories always move toward the sliding surface and do not diverge away. This condition is typically expressed using the Lyapunov stability approach. Mathematically given as:

$$\lim_{\varphi \to 0^-} \frac{d\varphi}{dt}\Big|_{u=1} > 0 \quad \text{and} \quad \lim_{\varphi \to 0^+} \frac{d\varphi}{dt}\Big|_{u=0} < 0 \quad (21)$$

This inequality ensures that the system state moves toward the sliding surface.

Where:

- If $\varphi > 0$ and $\frac{d\varphi}{dt} < 0$, the system must decrease toward the surface.
- If $\varphi < 0$ and $\frac{d\varphi}{dt} > 0$, the system must increase toward the surface.

For the control action *u*:

- *u = 1* when the system state is below the sliding surface.
- *u = 0* when the system state is above the sliding surface.

This switching action forces the system trajectory toward the sliding manifold, ensuring robust and stable operation.

Substituting the equation (17) in (21), the following two relations (22) and (23) can be

written as:

$$\lim_{\varphi \to 0^-} \frac{d\varphi}{dt} = \frac{\alpha(i_{Line} - i_{L)}}{C} + \frac{\beta(v_0 - v_i)}{L} > 0 \quad (22)$$

$$\lim_{\varphi \to 0^+} \frac{d\varphi}{dt} = \frac{\alpha(i_{Line} - i_{L)}}{C} + \frac{\beta(v_0)}{L} < 0 \quad (23)$$

Both equations (22) and (23) need to be satisfied to ensure the reachability conditions for the system under consideration.

Sliding Mode Dynamics:

In the Laplace domain, the differential equations (14) and (15) impose closed-loop features of the system. Taking the Laplace transform of the equation (14)

$$s.v_o(s) = \frac{i_L(s) - i_{Line}(s)}{C} \quad (24)$$

After simplifying, equation (24) results in equation (25).

$$i_L(s) = i_{Line}(s) + C.s.v_o(s) \quad (25)$$

Similarly, taking the Laplace transform of equation (16) results in (26).

$$\alpha[v_{ref}(s) - v_0(s)] + \beta[i_{ref}(s) - i_{Line}(s)] \quad (26)$$

Substituting the value of $i_L(s)$ From equation (25) and equating it to zero results in equation (27).

$$v_o(s)[\alpha + \beta.C.s] = \alpha v_{ref}(s) + \beta i_{ref}(s) - \beta i_{Line}(s) \quad (27)$$

In the Laplace domain, the equation (27) expresses the closed-loop dynamic behavior of the system. Now as it is evident that the load imposes the constant reference value, the final relation can be written as:

$$\frac{v_o(s)}{i_{Line}(s)} = \frac{-\beta}{\alpha + \beta.C.s} \quad (28)$$

Equation (28) represents the closed-loop dynamics of the DC microgrid system in the Laplace domain.

Proposed Distributive Architecture:

This paper proposes an IoT-based distributive control architecture for the minimization of circulating current among parallel connected sources and ensuring voltage regulation in a DC microgrid. The proposed architecture is shown in Fig. 7. Each source controller communicates with the other source controller through an IoT communication link, and in this way, the value of the current shared by each source (per unit) is communicated to all the sources. Based on this knowledge, the controller of each source calculates the average current value shared by all the sources which is given in equation (29).

$$i_j^{avg} = \frac{\sum_{j=1}^{n} i_j^{pu}}{n} \quad (29)$$

Here i_j^{pu} Is the source-j current (in per unit)? As the load changes, the deterioration in voltage regulation is restored as the new values of current are communicated between the sources. A flow diagram of the complete process is shown in Figure. 8.

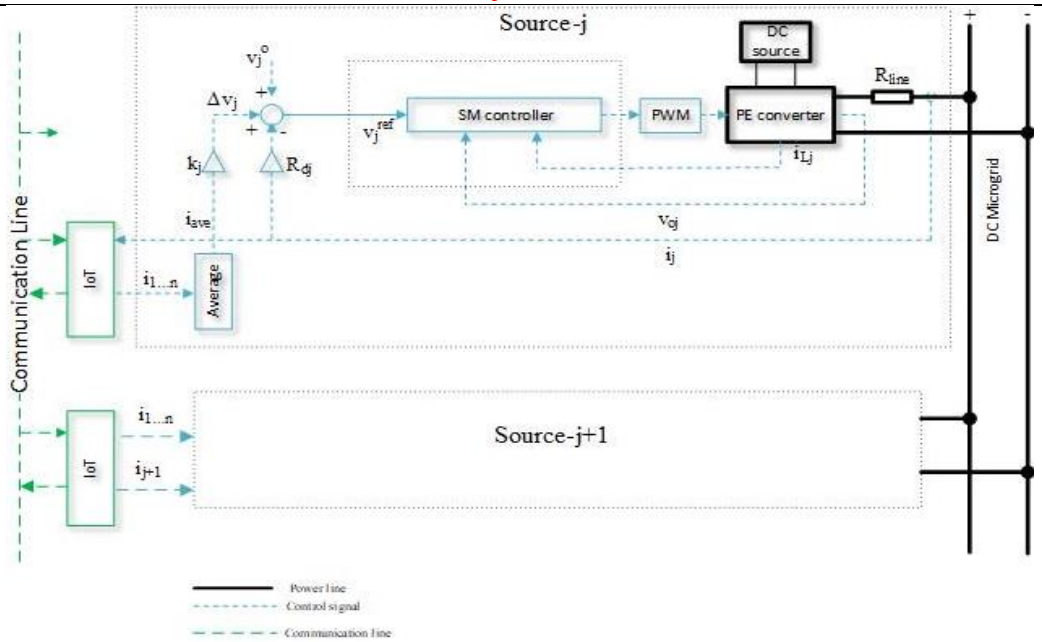

Figure 7 SMC with distributive architecture for parallel-connected DC microgrid.

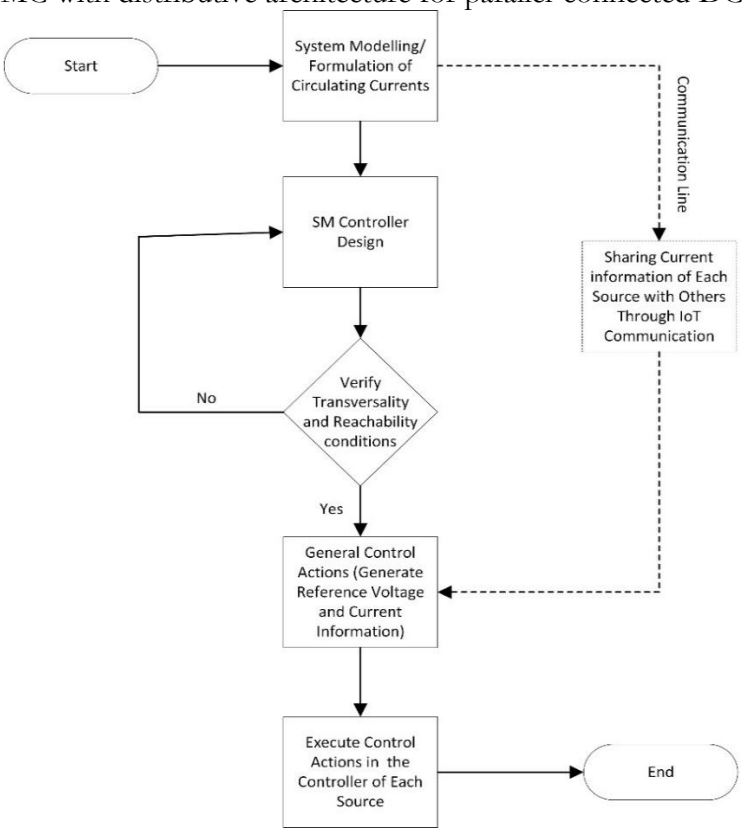

Figure 8 Complete Flow Diagram of the Methodology.

Result and Discussion:

The results from the MATLAB/Simulink simulations highlight the limitations of conventional PI control techniques in managing circulating currents and ensuring proper current sharing among sources. The system's efficiency is evaluated by first simulating a DC microgrid with only two sources with specifications given in Table 2 utilizing conventional PI-based control methods, including voltage loop and cascaded voltage-current loop control, and results are summarized below.

Table 2 Parameters of DC microgrid

Item	Parameter	Value
Converter 1	Inductor, L1	110mH
	Capacitance, C1	500 µF
	Proportional Gain Kp1	10
	Integral Gain Ki1	0.1
Converter 2	Inductor, L2	110 mH
	Capacitance, C2	500 µF
	Proportional Gain Kp2	10
	Integral Gain Ki2	0.1
Cable 1 Resistance	R1	0.25 Ω
Cable 2 Resistance	R2	1.25 Ω
Load	RL	22 Ω
Input Voltage	Vin	200 V
Nominal Voltage	Vout	120 V

1. **Voltage Loop PI Control:**

- Significant circulating currents (1.7A) arise due to uneven current distribution.
- Converter 1 supplies 4.355A, while converter 2 provides only 0.972A, disrupting the load-sharing balance.

2. **Cascaded Voltage & Current PI Control:**

- Some improvement in circulating current reduction (1.6A), but still not ideal.
- Converter 1 supplies 4.302A, while converter 2 contributes only 1.084A.

The results mentioned above highlight that both methods fail to minimize circulating currents among sources. Additionally, a trade-off between current sharing and voltage regulation is observed, showing that traditional methods fail to optimize both simultaneously.

To compare the performance of the proposed IoT-based distributive SM controller, the same DC microgrid is simulated utilizing the proposed method, and the results of the performance comparison are given below.

Performance Comparison:

1. **PI-Based Voltage Control:**

- Circulating current: 1.7A (high).
- Unequal sharing: 4.355A (Converter 1) vs. 0.972A (Converter 2).

2. **PI-Based Cascaded Voltage & Current Control:**

- Circulating current: 1.6A (slightly improved).
- Unequal sharing: 4.302A (Converter 1) vs. 1.084A (Converter 2).

3. **Proposed IoT-Based SM Control:**

- Circulating current: 0.03941A (almost negligible).
- Equal sharing: 2.721A (Converter 1) vs. 2.642A (Converter 2).

The results validate that the proposed SM controller outperforms traditional PI-based methods by:

1. Minimizing Circulating Currents – SM control reduces circulating currents to nearly zero.
2. Ensuring Balanced Load Sharing – Both sources contribute proportionally.
3. Maintaining Excellent Voltage Regulation – Stable operation even with variations in line resistance.

Performance Comparison:

Control Method	Circulating Current	Current Sharing	Voltage Regulation
PI Voltage Loop	High (1.7A)	Unbalanced	Within Limits
Cascaded PI Control	Moderate (1.6A)	Still Unbalanced	Within Limits

Proposed SM Controller	Minimal (0.03941A)	Balanced	Excellent

Thus, the distributive SM controller is an efficient solution for mitigating circulating currents, improving current-sharing accuracy, and maintaining precise voltage regulation in DC microgrids.

Conclusion:

To address the ongoing energy crisis, RESs can be integrated into DC or AC microgrids based on specific requirements. DC microgrids hold significant promise due to their advantages, such as the absence of skin effect, reactive power complications, frequency synchronization issues, and lower inter-energy conversion losses.

A critical challenge in DC microgrids is ensuring precise current sharing among parallel-connected Distributed Energy Resources (DERs). Variations in output voltage, converter currents, and cable resistances can lead to circulating currents, which degrade overall voltage regulation and system efficiency.

To address this issue, this paper proposes an IoT-based distributive SM control architecture. The system's efficiency is evaluated by first simulating conventional PI-based control methods, including voltage loop and cascaded voltage-current loop control. The results highlight a trade-off between current sharing and voltage regulation, showing that traditional methods fail to optimize both simultaneously.

In contrast, the proposed SM controller effectively minimizes circulating currents, ensures a proper current-sharing ratio, and maintains excellent voltage regulation. The results demonstrate the superiority of the proposed technique, making it a robust solution for enhancing stability and efficiency in DC microgrids.

Limitations and Future Work:

SM controller is a robust control technique that is used for variable structured systems. The limitation of the SM technique is the infinite frequency requirement, which is practically not possible. So, it produces chattering phenomena during the sliding surface.

For recommendations in the future, there is a need to explore the SM techniques used for chattering reduction. Additionally, to implement SM controllers in hardware, modern high-processing tools are recommended to be explored for the said application.

Acknowledgment: The authors would like to especially thank The University of Lahore (UOL) and the University of Gujrat (UOG) for supporting and providing the environment for the research.

Author's Contribution: Muhammad Sharjeel Sarwar contributed to the literature review and system design. Muhammad Rashad contributed to the analysis and wrote the paper. Tayybah Kiren, Nazam Siddique, Bilal Ishfaq Ahmed, and Adeel Ahmed contributed to data collection and analysis tools. Muhammad Wasif and Muhammad Jehanzeb Irshad contributed to the presentation of the data and results.

Conflict of Interest: The authors declare no conflict of interest in publishing this manuscript.

Project details: This research study received no external funding. All the resources consumed were internally available.

References:

[1] Rinkesh, "Causes, Effects and Solutions to Global Energy Crisis - Conserve Energy Future," Conserve Energy Future. Accessed: Mar. 12, 2025. [Online]. Available: https://www.conserve-energy-future.com/causes-and-solutions-to-the-global-energy-crisis.php

[2] R. S. Manieniyan V, Thambidurai Muthuvelan, "STUDY ON ENERGY CRISIS AND THE FUTURE OF FOSSIL FUELS," Proceedings of SHEE 2009. Accessed: Mar. 12, 2025. [Online]. Available: https://www.researchgate.net/publication/267439286_STUDY_ON_ENERGY_CRISIS_AND_THE_FUTURE_OF_FOSSIL_FUELS

[3] R.E.H. Sims, "Renewable energy: a response to climate change," *Sol. Energy*, vol. 76, no. 1–3, pp. 9–17, 2004, doi: https://doi.org/10.1016/S0038-092X(03)00101-4.

[4] Ibrahim Dincer, "Renewable energy and sustainable development: a crucial review," *Renew. Sustain. Energy Rev.*, vol. 4, no. 2, pp. 157–175, 2000, doi: https://doi.org/10.1016/S1364-0321(99)00011-8.

[5] L. Xuan and S. Bin, "Microgrids - An integration of renewable energy technologies," *2008 China Int. Conf. Electr. Distrib. CICED 2008*, 2008, doi: 10.1109/CICED.2008.5211651.

[6] M. Shahbazitabar, H. Abdi, H. Nourianfar, A. Anvari-Moghaddam, B. Mohammadi-Ivatloo, and N. Hatziargyriou, "An Introduction to Microgrids, Concepts, Definition, and Classifications," *Power Syst.*, pp. 3–16, 2021, doi: 10.1007/978-3-030-59750-4_1.

[7] B. A. A. PCS183032, "PWM Based Fixed Frequency Equivalent SM Controller for Stability of DC Microgrid System," *J. Eng. Res.*, Accessed: Mar. 12, 2025. [Online]. Available: https://www.academia.edu/101842265/PWM_Based_Fixed_Frequency_Equivalent_SM_Controller_for_Stability_of_DC_Microgrid_System

[8] M. Rashad, M. Ashraf, A. I. Bhatti, and D. M. Minhas, "Mathematical modeling and stability analysis of DC microgrid using SM hysteresis controller," *Int. J. Electr. Power Energy Syst.*, vol. 95, pp. 507–522, 2018, doi: https://doi.org/10.1016/j.ijepes.2017.09.001.

[9] J. E. M. Michele Cucuzzella, Jacquelien M. A. Scherpen, "Microgrids control: AC or DC, that is not the question," *EPJ Web Conf*, vol. 310, p. 20, 2024, doi: https://doi.org/10.1051/epjconf/202431000015.

[10] P. W. Marcos Gomez-Redondo, Marco Rivera, Javier Muñoz, "A Systematic Literature Review on AC Microgrids," *Designs*, vol. 8, no. 4, p. 77, 2024, doi: https://doi.org/10.3390/designs8040077.

[11] V. A. Jaynendra Kumar, Anshul Agarwal, "A review on overall control of DC microgrids," *J. Energy Storage*, vol. 21, pp. 113–138, 2019, doi: https://doi.org/10.1016/j.est.2018.11.013.

[12] U. R. Muhammad Rashad, "Equivalent SM Controller for Load-Sharing and Dynamic Performance in a DC Microgrid Application," *Math. Probl. Eng.*, 2022, doi: https://doi.org/10.1155/2022/9700915.

[13] V. J. Thottuvelil and G. C. Verghese, "Analysis and control design of paralleled DC/DC converters with current sharing," *Conf. Proc. - IEEE Appl. Power Electron. Conf. Expo. - APEC*, vol. 2, pp. 638–646, 1997, doi: 10.1109/APEC.1997.575646.

[14] Y. Huang and C. K. Tse, "Circuit theoretic classification of parallel connected dc-dc converters," *IEEE Trans. Circuits Syst. I Regul. Pap.*, vol. 54, no. 5, pp. 1099–1108, 2007, doi: 10.1109/TCSI.2007.890631.

[15] S. Anand, B. G. Fernandes, and J. M. Guerrero, "Distributed control to ensure proportional load sharing and improve voltage regulation in low-voltage DC microgrids," *IEEE Trans. Power Electron.*, vol. 28, no. 4, pp. 1900–1913, Apr. 2013, doi: 10.1109/TPEL.2012.2215055.

[16] A. P. N. Tahim, D. J. Pagano, E. Lenz, and V. Stramosk, "Modeling and Stability Analysis of Islanded DC Microgrids under Droop Control," *IEEE Trans. Power Electron.*, vol. 30, no. 8, pp. 4597–4607, 2015, doi: 10.1109/TPEL.2014.2360171.

[17] S. Luo, Z. Ye, R. L. Lin, and F. C. Lee, "Classification and evaluation of paralleling methods for power supply modules," *PESC Rec. - IEEE Annu. Power Electron. Spec. Conf.*, vol. 2, pp. 901–908, 1999, doi: 10.1109/PESC.1999.785618.

[18] J. Rajagopalan, K. Xing, Y. Guo, F. C. Lee, and B. Manners, "Modeling and dynamic analysis of paralleled dc/dc converters with master-slave current sharing control," *Conf.*

Proc. - IEEE Appl. Power Electron. Conf. Expo. - APEC, vol. 2, pp. 678–684, 1996, doi: 10.1109/APEC.1996.500513.

[19] M. S. Sadabadi, N. Mijatovic, J. F. Tregouet, and T. Dragicevic, "Distributed Control of Parallel DC-DC Converters Under FDI Attacks on Actuators," *IEEE Trans. Ind. Electron.*, vol. 69, no. 10, pp. 10478–10488, Oct. 2022, doi: 10.1109/TIE.2021.3123613.

[20] J. G. Sebastian Trip, Renke Han, Michele Cucuzzella, Xiaodong Cheng, Jacquelien Scherpen, "Distributed Averaging Control for Voltage Regulation and Current Sharing in DC Microgrids: Modelling and Experimental Validation," *IFAC-PapersOnLine*, vol. 21, no. 23, pp. 242–247, 2018, doi: https://doi.org/10.1016/j.ifacol.2018.12.042.

[21] B. A. A. Muhammad Rashad, Uzair Raoof, Muhammad Ashraf, "Proportional Load Sharing and Stability of DC Microgrid with Distributed Architecture Using SM Controller," *Math. Probl. Eng.*, 2018, doi: https://doi.org/10.1155/2018/2717129.

[22] A. Nawaz, J. Wu, and C. Long, "Mitigation of circulating currents for proportional current sharing and voltage stability of isolated DC microgrid," *Electr. Power Syst. Res.*, vol. 180, p. 106123, 2020, doi: https://doi.org/10.1016/j.epsr.2019.106123.